Pure Appl. Chem., Vol. 77, No. 6, pp. 1009–1018, 2005.
DOI: 10.1351/pac200577061009

Fluorescence sensor applications as detectors for DNA damage, free radical formation, and in microlithography*

J. C. Scaiano‡, C. Aliaga, M. N. Chrétien, M. Frenette, K. S. Focsaneanu, and L. Mikelsons

Department of Chemistry, University of Ottawa, 10 Marie Curie, Ottawa, Ontario K1N 6N5, Canada

Abstract: Fluorescence sensors have been developed to monitor radical reactions, DNA damage, acid-catalyzed processes, detection of electron-deficient molecules, and zeolite applications. The examples presented emphasize applications in polymer and supramolecular systems.

Keywords: photochemistry; fluorescence; sensors; free radicals; DNA damage; lithography; pyrene.

INTRODUCTION

This contribution deals with fluorescence-based sensing methods studied in our group during the last few years. Many group members, past and present, have contributed material, and their names appear in the references; this paper is coauthored by current group members whose recent contributions are emphasized in this article.

The high sensitivity of fluorescence methods, along with the ease of detection and the availability in our laboratories of both steady-state and time-resolved techniques, have frequently dictated the selection of chromophores. Due to space restrictions for this contribution, we concentrate on the chemical aspects with only passing mentions of the experimental techniques that are described in the original articles.

PREFLUORESCENT PROBES

We describe as *prefluorescent probes* molecules that are essentially nonfluorescent, but become luminescent when a selected chemical event takes place. In our examples, these events frequently involve free radical reactions. The molecules used consist of a fluorescent chromophore tethered to a paramagnetic group, normally a persistent nitroxide, as illustrated in Scheme 1. Trapping of a free radical generates a diamagnetic alkoxyamine, and in the process restores the fluorescent properties of the fluorophore.

Prefluorescent probes as radical sensors

The following examples illustrate the use of the sensors in Scheme 1 for the detection of free radicals in polymerization reactions, in thin films, and in supramolecular systems.

---

*Paper based on a presentation at the XXth IUPAC Symposium on Photochemistry, 17–22 July 2004, Granada, Spain. Other presentations are published in this issue, pp. 925–1085.
‡Corresponding author

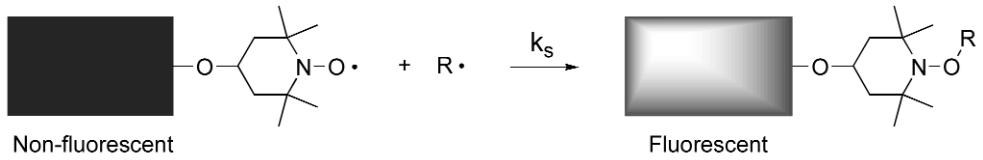

Scheme 1 The fluorescence emission of the fluorophore (rectangle) is quenched by the nitroxide moiety, but is restored when a free radical (R•) is scavenged.

Living free radical polymerization

Our first application of these probes involved the study of polymers terminated by coupling of a carbon-centered radical with a nitroxide radical [1]. The resulting alkoxyamine is effectively a dormant polymer. At the appropriate temperature (typically 90–140 °C for polystyrene), the weak O–C bond can be cleaved, leading to free radicals; if monomer is available, the polymer-based carbon-centered radical is then able to continue polymer growth until "recapping" takes place. If a modified nitroxide is present (such as a prefluorescent probe), recapping leads to a fluorescent polymer. The growth in fluorescence intensity can be used to determine the relevant rate constants for the system, and from them the bond dissociation energy (BDE). For the system of Scheme 2, the C–O BDE was calculated as 28.4 kcal/mol.

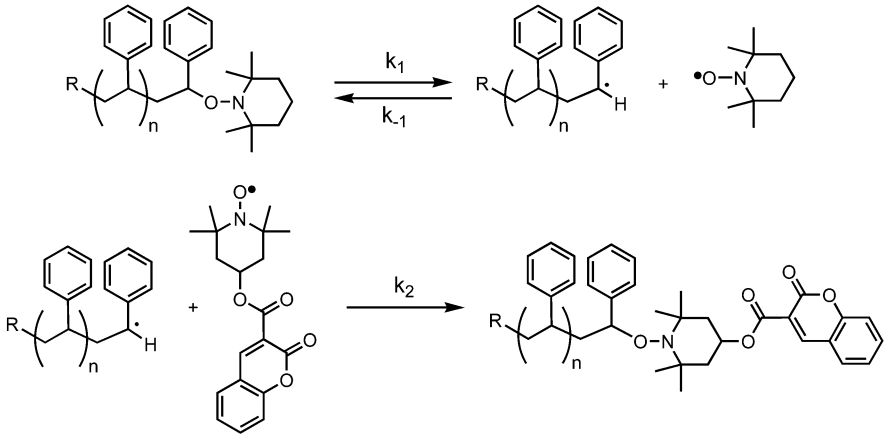

Scheme 2 Nitroxide (TEMPO) trapping of the polystyrene radical that mediates living free radical polymerization. Trapping by the prefluorescent probe leads to the fluorescent alkoxyamine.

Radicals in thin films

In another example, prefluorescent radical probes and photoinitiators were used to detect radical generation in polymer films using fluorescence spectroscopy and microscopy [2]. Prefluorescent radical probes are the foundation of a fluorescence imaging system for polymer films, which may serve both as a mechanistic tool in the study of photoinitiated radical processes in polymer films and in the preparation of functional fluorescent images. An example using a coumarin-derived probe is illustrated in Fig. 1.

Radicals in supramolecular systems

Prefluorescent probes can also be used to monitor dynamic radical processes occurring in heterogeneous systems such as zeolites. Zeolites are crystalline aluminosilicates comprised of a three-dimensional array of pores with well-defined cavity and aperture sizes. In one recent example, we used a prefluorescent probe based on the dansyl fluorophore to monitor carbon-centered radical behavior within the pores of faujasite zeolite NaY [3]. The dansyl-TEMPO probe (DT) used for these studies

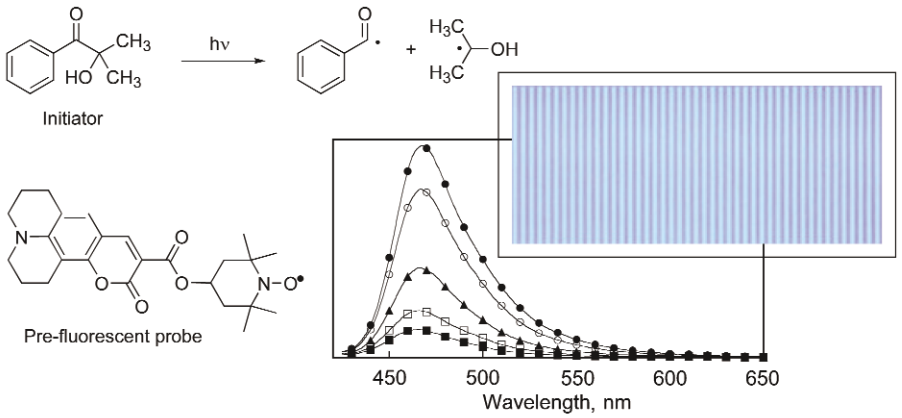

Fig. 1 Fluorescence spectra of a 2.3-µm-thick PMMA film containing initiator (0.5 wt %) and probe (5 wt %) at 0 s (■), 15 s (□), 30 s (▲), 45 s (○), and 60 s (●) of 360-nm exposure, obtained by excitation at 410 nm. The radicals are generated by photolysis of a commercial benzoin, and the image was recorded with a fluorescence microscope using a 2.3-µm-thick PMMA film exposed through a mask with 10-µm line spacing for 90 s [2].

(Scheme 3) is too large to be included directly into the zeolite through the ~7.4 Å windows and so must be synthesized within the pores via a process called ship-in-a-bottle synthesis [4]. As the name suggests, synthesis of the probe is accomplished by first including the smaller precursor molecules (dansyl chloride and 4-amino TEMPO) into the cavity followed by catalyzed formation of the desired product, the product is permanently entrapped in the pore in which it was formed due to its large size.

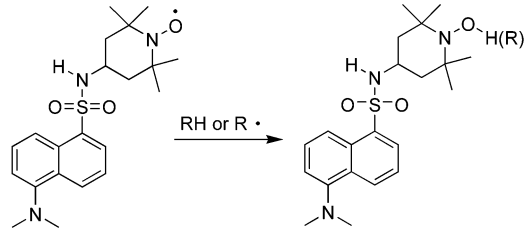

Scheme 3 Reaction of DT with a free radical or hydrogen donor to generate a fluorescent alkoxyamine or hydroxylamine.

We used DT encapsulated in NaY (DT@Y) to monitor radicals formed inside zeolite particles (Scheme 3). Since DT@Y is trapped and immobile within the pore, monitoring the fluorescence increase with respect to time allows us to visualize the diffusion of radicals through the porous solid. In one representative example, 2,2'-azobisisobutyronitrile (AIBN) was co-included in the zeolite, and, following heating, an increase in fluorescence intensity over time is observed as the radicals diffuse through the pores, encounter the embedded probe, and subsequently undergo a coupling reaction to generate the fluorescent product (Fig. 2.)

Other processes investigated using this probe include the penetration and diffusion of carbon-centered radicals generated *outside* of the zeolite particle and the interaction between the embedded probe and molecules that are good hydrogen donors [3].

Prefluorescent probes as a tool for antioxidant properties

Chain-breaking antioxidant action is based on the trapping of radicals involved in the oxidative chain by efficient hydrogen-transfer processes. In this work, we evaluated the ability of 4-(3-hydroxy-2-

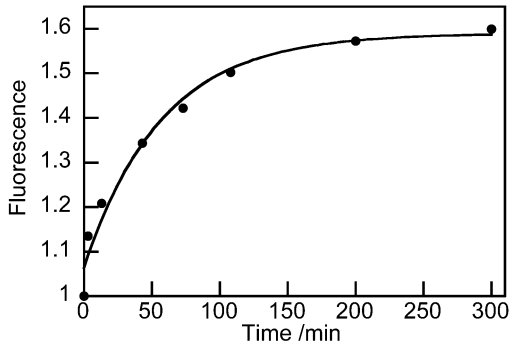

Fig. 2 Fluorescence growth (normalized to 1.0 at $t = 0$) measured after heating a solid sample of DT@Y with co-included AIBN (λ_{ex} = 305 nm, λ_{mon} = 550 nm).

methyl-4-quinolinoyloxy)-2,2,6,6 tetramethylpiperidine-1-oxyl free radical (QT), a prefluorescent TEMPO probe, to monitor hydrogen transfer from reactive phenols (Scheme 4).

There are literature precedents for the fast reaction of nitroxide radicals with ubiquinol-9, phenolic, and thiol antioxidants [5,6]. Other studies have shown a very slow reaction between TROLOX and TEMPOL (4-hydroxy-TEMPO) in aqueous solvents, suggesting that traces of metal ions could catalyze the reaction [7]. In the absence of metal ions, the kinetics of this process are believed to reflect hydrogen transfer.

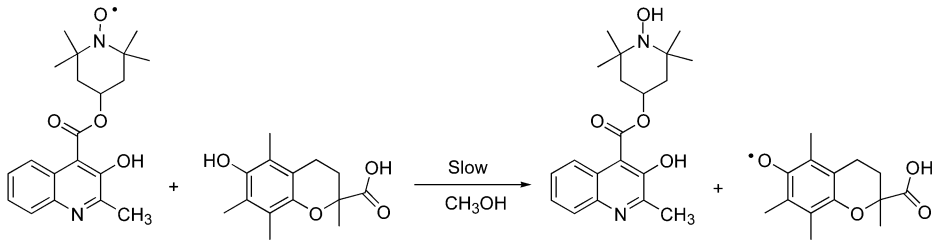

Scheme 4 Prefluorescent probes can abstract hydrogen from some hydrogen donors, such as TROLOX in this example.

The mechanism by which this prefluorescent nitroxide probe works has been explained above. In this case, the fluorescence is restored when the nitroxide moiety is trapped by a hydrogen donor to produce the diamagnetic hydroxylamine (QTH). We have used QT as a probe mimicking peroxyl radical reactivity [8] in order to evaluate the antioxidant activity of phenolic compounds and to obtain kinetic parameters involved in the hydrogen-transfer process. Rate constants for TROLOX (0.2 M^{-1} s^{-1}), gallic acid (4.6×10^{-3} M^{-1} s^{-1}), and BHT (3.3×10^{-3} M^{-1} s^{-1}) were obtained in methanol. Experiments performed in deuterated solvents gave an isotope effect of 10.5 for TROLOX, whereas a factor of 4 was obtained for gallic acid, confirming that a hydrogen-transfer process is the dominant mechanism. While large, values of this magnitude for reactions of phenols have been known for over 40 years [9]. Interestingly, the rate constants for TROLOX are essentially the same in water and in methanol; product stabilization in the former probably compensates for reactivity reductions due to stronger hydrogen bonding. However, the rate constant observed for gallic acid (a polyphenol) in buffer (8.9×10^{-3} M^{-1} s^{-1}) is larger than in methanol (4.6×10^{-3} M^{-1} s^{-1}). The fact that the less reactive substrate (gallic acid) shows a smaller isotope effect suggests that some degree of charge transfer may be involved in this example, probably mediated by the deprotonation of the acidic group.

DPPH (2,2-diphenyl-1-picrylhydrazyl), a persistent free radical, has close to a half-century history of use as a probe for radical reactions with phenols [10]. Despite this, there are concerns in rela-

tion to the value of kinetic parameters determined with DPPH in hydrogen-bonding solvents [11]. This is in part related to the strongly electron-deficient radical center in DPPH. Nitroxide radicals, while electrophilic (most oxygen-centered radicals are), are not as electron-deficient as DPPH, and thus are better model systems. Prefluorescent probes provide a convenient approach for determination of the hydrogen-donor ability of phenols; the method is very sensitive and appears less prone to suffer from the problems of highly electron-deficient probes such as DPPH.

DETECTION OF DNA DAMAGE

When DNA is exposed to radiation, damage is induced, which results in a weakened polymer structure. In order to quantify DNA damage, a protocol is required for selectively unwinding damaged DNA without affecting intact DNA. When damaged DNA undergoes the appropriate treatment protocol, the damaged sites can result in strand scissions, causing unwinding of the DNA. DNA damage can then be quantified by measuring the ratio of single-stranded (ss) to double-stranded (ds) DNA.

A recent technique for determining ss-to-dsDNA ratios in solution involves the measurement of the preexponential factors in the fluorescence decay traces of dye-DNA complexes [12]. When the DNA-stain dye PicoGreen® (PG) is free in solution, it can dissipate its excitation energy by rotation around its central methine bridge, but when it is intercalated between the base pairs of DNA, its fluorescence yield is quite high. This large increase in quantum yield upon binding to dsDNA as compared to free in solution reflects the inefficiency of radiationless processes. The PG-ssDNA complex is less rotationally restricted than the PG-dsDNA complex and should exhibit a different fluorescence lifetime. It was found that the PG-dsDNA complex followed a monoexponential fluorescence decay with a lifetime of about 4 ns [12]. The PG-ssDNA complex exhibited a biexponential decay with an average lifetime of 2 ns. Using this information, it is possible to derive an equation where the only unknown is the amount of dsDNA in a sample, thus making it possible to quantify the ratio of ss-to-dsDNA, and hence DNA damage, since the percentage of ssDNA is a direct measure of DNA damage. The beauty of this technique lies in the fact that the fluorescence lifetime is an intensive property, i.e., it is independent of the amount of fluorophore and it is unique for a dye within a given environment, and thus blanks are not required.

PG fluorescence lifetimes have been used to establish DNA damage in sheep white blood cells following gamma radiation in the 0–100 Gray (Gy) range [13]. Once the fluorescence lifetime was determined, the ratio of ss-to-dsDNA was calculated, giving the percentage of ssDNA and hence the amount of radiation exposure. A dose of 1 Gy produces 1000 ss breaks and 40 ds breaks in the DNA of one cell [14]. When studying DNA damage, conditions must be used that unwind damaged DNA while leaving undamaged DNA intact. Work from our laboratory has established the best conditions for selective unwinding, typically involving alkali treatment.

Many of the foods that we eat are irradiated, in a process known as "cold pasteurization", in order to kill bacteria, eliminate parasites, improve product quality, and extend shelf life. Irradiated foods receive doses (usually gamma radiation) on the order of 1 kGy, or the equivalent of ~10^6 X-rays. This technique would make it possible to determine whether or not food has been irradiated, thus contributing to regulatory issues and truthful labeling.

IMAGING APPLICATIONS IN LITHOGRAPHY

We already illustrated one application of prefluorescent probes to the study of latent images in the field of microlithography. Our long-standing collaboration with industrial partners in this area has been reflected in several applications related to predevelopment detection of lithographic images. The ability to monitor latent images opens the door to material improvements that are more difficult to evaluate after the image has been developed.

The term "chemical amplification" is widely employed to describe lithographic processes where light exposure (frequently in the near or far ultraviolet region) leads to the photochemical generation of acid, which then acts as a catalyst to promote film dissolution (positive image) or polymer crosslinking leading to reduced solubility (negative image). One of the more common chemical reactions is the acid-catalyzed deblocking of *tert*-butoxycarbonyl (*t*BOC) protecting groups [15].

We have developed a sensor that takes advantage of the deblocking process mentioned above [16], but that upon deblocking generates a strongly fluorescent group. The sensor shown in Scheme 5 takes advantage of the fact that for coumarins, protection of the phenolic function leads to the suppression of its otherwise strong fluorescence.

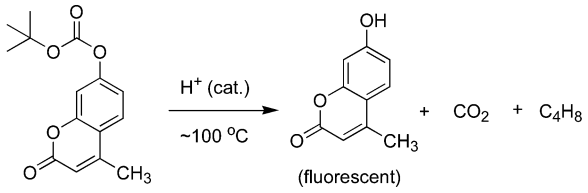

Scheme 5 Coumarin-based fluorescence sensor for *t*BOC deblocking by photogenerated acid.

This *t*BOC deblocking sensor gives us an inside view of a crucial step in lithography. Since fluorescence detection is highly sensitive, small amounts of prefluorescent sensor can be used to assess the deblocking of the surrounding resist material. Therefore, the introduced prefluorescent dyes act as non-intrusive reporters to confirm deblocking of the polymer resist via fluorescence imaging. This yields valuable information on the chemical transformations occurring in the resist, without the need to com-

Fig. 3 Fluorescent images in PMMA thin films using the prefluorescent probe of Scheme 5; line spacing is 55 μm, and film thickness is 1.43 μm.

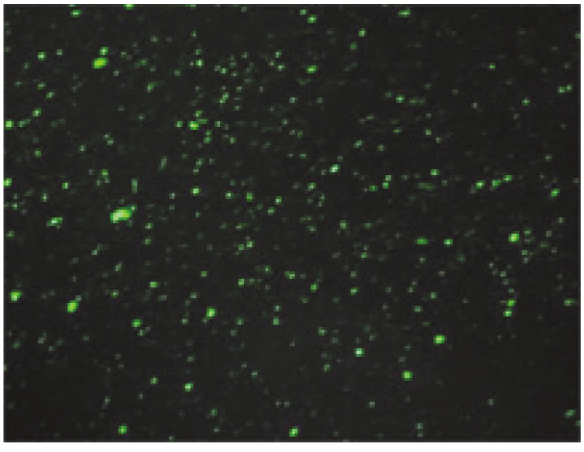

Fig. 4 Fluorescence microscopy image of F@HY suspended in aqueous media.

plete the development process. The increase in fluorescence can also be monitored in "real time" and thus serve to follow the time-dependent nature of deblocking processes. A fluorescent image using this technique is presented in Fig. 3 (see p. 1014) where the blue represents deblocked regions of the thin polymer film and the dark regions remain chemically untouched.

FLUORESCEIN ENCAPSULATED IN ZEOLITES

One of the projects in our group involves the development of *supramolecular sunscreens*, a concept that involves the encapsulation of common sunscreen molecules in the supercages of zeolites. These materials retain the sunblock properties of the active ingredient, while preventing their contact with skin. Further, the zeolite can act as a light scatterer, contributing to the sun protection properties of the material. As part of the development of these new materials, it became necessary to construct zeolite-incorporated sensors that could help evaluate the interaction between zeolites and skin cells.

When designing a zeolite based probe to monitor interactions in biological systems there are three main considerations: (1) the probe must have spectroscopic properties that are convenient for applications such as fluorescence microscopy, (2) the sensor itself must be nontoxic, and (3) the sensor must be permanently entrapped within the zeolite particle in order to prevent complications arising from fluorophore escape into the bulk media. In order to address these considerations, we chose to pursue the ship-in-a-bottle synthesis of fluorescein, a popular dye for biological applications. The concept of ship-in-a-bottle synthesis has been addressed in a previous section dealing with dansyl-TEMPO. Fluorescein is formed as a trapped moiety within the pores of faujasite zeolite HY following acid-catalyzed condensation of resorcinol and phthalic anhydride (Scheme 6) yielding the fluorescently labeled zeolite particles. The photophysical properties of this new material have been fully characterized. Interestingly, encapsulated fluorescein has a greatly enhanced photostability with respect to bleaching as compared to the probe in solution [17].

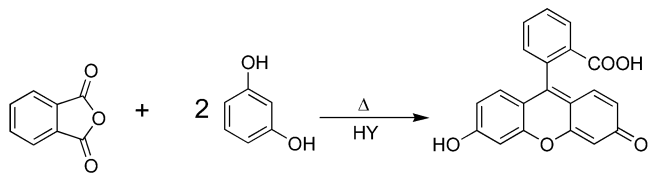

Scheme 6 Acid-catalyzed formation of fluorescein within the cavities of acidic zeolite HY.

Figure 4 (see p. 1014) shows the particles as they appear by fluorescence microscopy. In the context of cellular interactions, we can employ the technique of confocal fluorescence microscopy, where data is obtained at different planes within the sample, to determine whether or not the labeled particles have penetrated the cell.

PYRENE AS A SENSOR FOR ELECTRON-DEFICIENT MOLECULES

The equilibrium established between the monomer and excimer forms of pyrene in moderately concentrated solutions has been rigorously investigated [18]. However, the effect of certain quenchers on the ratio of the two species remains largely unexplored. We are currently developing a methodology that exploits this equilibrium to distinguish electron-poor from electron-rich compounds.

At concentrations greater than 0.001 M, the fluorescence spectrum of pyrene shows two distinct emissions. The fine structured bands at $\lambda < 400$ nm correspond to emission from the singlet excited state, ^{1}Py*. However, the broad band centered around 470 nm is emission due to the formation of "excited dimers", or excimers. The excimer ^{1}(Py-Py)* is a relatively stable complex between one excited molecule of pyrene and another in its ground state, Scheme 7 [19].

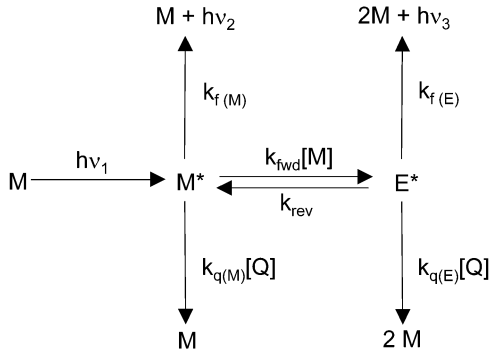

Scheme 7 Fluorescence quenching of the monomer (M) and excimer (E) forms of pyrene.

A variety of molecules are able to quench fluorescence emission from pyrene via charge- or electron-transfer mechanisms [20]. In our work, a series of compounds were used as quenchers, ranging from electron-rich to electron-poor molecules. It became apparent from the fluorescence spectra that each of the quenchers employed fell into one of three categories: nonquenchers, weak quenchers, and strong quenchers.

"Nonquenchers" are electron-rich compounds (e.g., trialkyl amines), where $k_q[Q]$ is very small; i.e., no significant quenching of pyrene is observed, even at high [Q].

"Weak quenchers" are typically aromatic amines (*N*,*N*-dimethyl-2,6-diisopropylaniline shown in Fig. 5, left), where $k_q[Q]$ is significant, yet small in comparison to the rates of excimer formation and dissociation, $k_{fwd}[M]$ and k_{rev}, respectively. Thus, the system remains in equilibrium, with excimer dissociating to replenish quenched monomer and vice-versa. This dynamic quenching is described by the normal Stern–Volmer equation:

$$\frac{\Phi_f^\circ}{\Phi_f} \approx \frac{F_\circ}{F} = 1 + k_q \tau_f^\circ [Q] = 1 + K[Q]$$

Since the equilibrium between the two forms is constantly maintained, and due to mass balance, the slopes of the Stern–Volmer plots for each form (i.e., the Stern–Volmer constants K_M and K_E) will be equivalent, as shown in the inset graph.

The electron-deficient compounds (nitrobenzene shown in Fig. 5, right) had monomer fluorescence quenching, which also followed the Stern–Volmer relationship. However, the excimer form

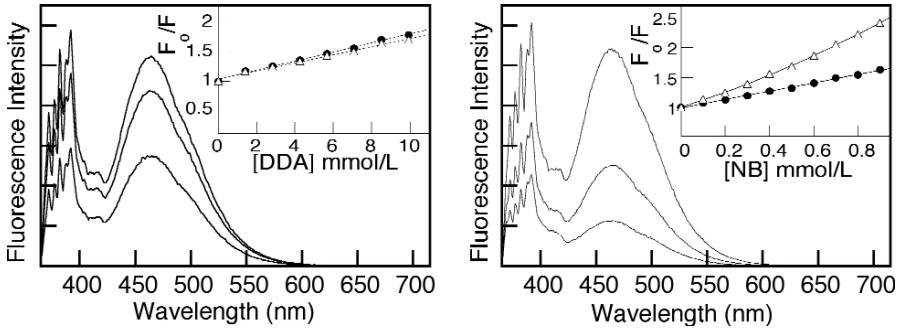

Fig. 5 Steady-state fluorescence quenching of pyrene (3 mM in 99 % ethanol). Left: Q = *N*,*N*-dimethyl-2,6-diisopropylaniline (DDA); Right: Q = nitrobenzene (NB). Insets: Stern–Volmer plots taken at 392 nm to represent the monomer form (●) and 464 nm to represent the excimer form (△). Note the differences in scale. Some spectra omitted for clarity.

showed a positive deviation from the expression. The compounds responsible for this deviation consisted primarily of nitroaromatics and were thus labeled "strong quenchers" due to their large bimolecular quenching rate constants.

Interestingly, the linear vs. nonlinear quenching of the monomer and excimer species (respectively) allows us to construct calibration curves by plotting the ratio of the fluorescence intensities of the two forms (F_M/F_E), as shown in Fig. 6. Consequently, quantification of unknown samples is now possible.

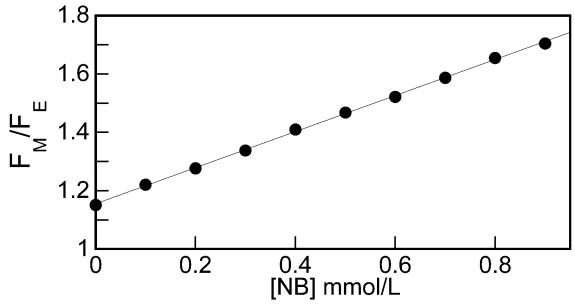

Fig. 6 Calibration curve for nitrobenzene; constructed by taking the ratio of fluorescence intensities at 392 and 464 nm.

Since explosive materials are primarily electron-deficient molecules (e.g., 2,4,6-TNT, RDX, and HMX), we are attempting to use the property illustrated in Fig. 6 as a tool for analytical detection methods. An example is modification of environmental or forensic sample analysis: currently, samples are generally analyzed according to the EPA8330 protocol developed by the U.S. Environmental Protection Agency [21]. In this method, samples are injected into a reverse-phase HPLC with UV–vis detection. Although sensitivity is high, it offers little selectivity toward explosives (electron-deficient compounds), especially when these compounds are part of complex matrices. The addition of a fluorescence spectrophotometer as a detection system has been explored and has been proven to be an effective method [22]: a fluorophore is introduced postcolumn via a mixing tee, and the resulting fluorescence quenching by separated components is monitored. However, the resulting chromatograms are derived from monitoring one emission wavelength only: by monitoring the ratio of monomer-to-excimer emission instead, it should be possible to highlight those peaks which are suspected explosives (nitrated compounds).

ACKNOWLEDGMENTS

We acknowledge the contribution of many past and present coworkers at the University of Ottawa, whose names appear in the references. This research has been supported by NSERC (Canada), the Canadian Foundation for Innovation, the Canadian Space Agency, R&H Electronic Materials, the Government of Ontario, and AFMnet.

REFERENCES

1. O. García Ballesteros, L. Maretti, R. Sastre, J. C. Scaiano. *Macromolecules* **34**, 6184–6187 (2001).
2. C. Coenjarts, O. García, L. Llauger, J. Palfreyman, A. L. Vinette, J. C. Scaiano. *J. Am. Chem. Soc.* **125**, 620–621 (2003).
3. A. Ricci, M. N. Chretien, J. C. Scaiano. *Chem. Mater.* **16**, 2669–2674 (2004).
4. J. C. Scaiano and H. García. *Acc. Chem. Res.* **32**, 783–793 (1999).

5. J. Fuchs, N. Groth, T. Herrling, G. Zimmer. *Free Rad. Biol. Med.* **22**, 967–976 (1997).
6. K. Hiramoto, N. Ojima, K. Kikurawa. *Free Rad. Biol. Med.* **27**, 45–53 (1997).
7. C. Aliaga, E. A. Lissi, O. Augusto, E. Linares. *Free Rad. Biol. Med.* **37**, 225–230 (2003).
8. C. Aliaga, A. Aspée, J. C. Scaiano. *Org. Lett.* **5**, 4145–4148 (2003).
9. J. A. Howard and K. U. Ingold. *Can. J. Chem.* **40**, 1851–1864 (1962).
10. A. F. Bickel and E. C. J. Kooyman. *J. Chem. Soc*. 2415–2416 (1957).
11. G. Litwinienko and K. U. Ingold. *J. Org. Chem.* **68**, 3433–3438 (2003).
12. G. F. Cosa, K.-S. Focsaneanu, J. R. N. McLean, J. C. Scaiano. *Chem. Commun.* 689–690 (2000).
13. G. Cosa, A. L. Vinette, J. R. N. McLean, J. C. Scaiano. *Anal. Chem.* **74**, 6193–6169 (2002).
14. J. F. Ward. *DNA Damage Produced by Ionizing Radiation in Mammalian Cells: Identifies, Mechanism of Formation, and Repairability*, Vol. 35, Academic Press, New York (1988).
15. S. A. MacDonald, C. G. Wilson, M. J. Frechet. *Acc. Chem. Res.* **27**, 151–158 (1994).
16. M. Frenette, C. Coenjarts, J. C. Scaiano. *Macromol. Rapid Comm.* **25**, 1628–1631 (2004).
17. M. N. Chretien, B. Shen, H. García, A. M. English, J. C. Scaiano. *Photochem. Photobiol.* **80**, 434–437 (2004).
18. J. B. Birks. *Photophysics of Aromatic Molecules*, Wiley-Interscience, London (1970).
19. A. Gilbert and J. Baggott. *Essentials of Molecular Photochemistry*, Blackwell, Oxford (1991).
20. J. R. Lakowicz. *Principles of Fluorescence Spectroscopy*, 2nd ed., Kluwer Academic, New York (1999).
21. C. A. Weisberg and M. L. Ellickson. *Am. Lab.* **30**, 32N–32V (1998).
22. J. V. Goodpaster and V. L. McGuffin. *Anal. Chem.* **73**, 2004–2011 (2001).